JOURNAL OF PLANKTON RESEARCH | VOLUME 26 | NUMBER 4 | PAGES 433–443 | 2004

Light as an information carrier underwater

MARIA RAGNI* AND MAURIZIO RIBERA D'ALCALÀ
STAZIONE ZOOLOGICA 'A. DOHRN', VILLA COMUNALE, 80121, NAPLES, ITALY

*CORRESPONDING AUTHOR: ragni@szn.it

Light is a source of both energy and information for the biota. The spatial, temporal and spectral variability of light experienced by marine phytoplankton differs significantly from that experienced by terrestrial plants, due to the selective attenuation of solar irradiance in the aquatic medium. In the present study we analysed such variability and focused, in particular, on those bands within the spectrum that may act as potential signals for physiological responses. Our results demonstrate that the spectral variation of the light field carries information on the time of day, the vertical position and the presence of very close neighbours, also underwater. This is consistent with the recent findings of a widespread occurrence of photoreceptors in marine algae. We show also that red photoreceptors, whose presence in marine algae was difficult to reconcile with the strong attenuation of long wavelengths by water, may be triggered at depth by the red light generated by transpectral processes.

INTRODUCTION

Light availability and its spectral distribution are first-order controls on the productivity of the sea. Photoautotrophs use light as a source of energy for their biosynthesis; however, several other responses and behaviours such as complementary chromatic adaptation (Grossmann *et al.*, 1993), vertical migrations (Cullen *et al.*, 1985), phototaxis (Sineshchekov *et al.*, 2000), chloroplast movement and reorientation (Furukawa *et al.*, 1998), circadian rhythms (Sournia, 1974), and certain aspects of life strategies (Eilertsen *et al.*, 1995) are also regulated by light. Therefore, the reconstruction of the spatial and temporal variability of the underwater light field and its spectral signature can be considered essential prerequisites for the understanding of phytoplankton physiology, ecology and behaviour.

Phytochromes of higher plants are involved in controlling and modulating physiological and developmental responses and are believed to have been selected for interpreting light signals in terrestrial environments. However, the presence of this family of photoreceptors in the earliest marine organisms, such as cyanobacteria and purple bacteria, supports the hypothesis of a marine origin of phytochrome. Indeed, algae physiologically acclimate to variations in spectral quality (Senger and Bauer, 1987), and several chromatic photoreceptors, such as red:far-red-light (R:FR) absorbing photoreceptors (Wu and Lagarias, 1997; Jorissen *et al.*, 2002), UV and blue (B) light photoreceptors (Hader and Lebert, 1998), and green (G) light photoreceptors (Sineshchekov and Govorunova, 2001) have been reported in different phytoplankton groups.

Some authors have proposed that band ratios (e.g. R:FR, B:R and G:R) may act in algae, as in higher plants, as complex switches controlling relevant processes such as synthesis or destruction of pigments (Lopez-Figueroa, 1992), migration (Lopez-Figueroa, 1998), photoadaptation and phototaxis. By contrast, some other authors (Hughes *et al.*, 1984; Dring, 1988) have stated that in aquatic environments light intensity is far more important than light quality in regulating photoacclimation and other physiological responses, because of the high degree of variability of spectral ratios with depth. In addition, given the high rate of attenuation of red wavelengths with depth, one could exclude the possibility that red light may play a role below the first few metres of the water column.

During the last two decades a large effort has been devoted to the characterization of the bio-optical properties of the water column, both with measurements and models (Morel, 1988, 1991; Sathyendranath and Platt, 1988). The wide range of existing bio-optical models has been largely applied so far either to the quantification of photosynthesis or to the reconstruction of the spectral signatures of the ocean as a diagnostic tool for biogeochemical processes in the sea. There has been little effort, however, to estimate the variability of the underwater light field in order to predict photobiological responses and activities of marine organisms.

doi: 10.1093/plankt/fbh044, available online at www.plankt.oupjournals.org

To address this problem, we discuss here the results derived from a semi-analytical radiative transfer model, to reconstruct spectral irradiance at the sea surface and in the pelagic realm; the results are used to identify specific bands and band ratios suited for photoregulative responses in marine algae, also given the recent evidence of the spectral response of specific phytoplankton photoreceptors (Wu and Lagarias, 1997; Furukawa *et al.*, 1998; Kondou *et al.*, 2001).

METHOD

The amplitude and variability in spectral irradiance are predicted over the visible bands, where specific photoreceptors are active, by using a semi-analytical radiative transfer model. In particular we focus on the absorption bands of known and putative photoreceptors of algae, such as cryptochrome (B, ~450 nm), rhodopsin (G, ~500 nm) and phytochrome-like receptors (R and FR, 670 and 730 nm).

We compute with the model the spectral downwelling irradiance at the ocean surface and in the ocean interior. The model inputs include the geographical location, date, time, and a range of environmental parameters. Its structure is based principally on pre-existing models, as described below, but has been modified to address the potential for photoregulation responses by marine phytoplankton.

Solar radiation at the sea surface

The intensity of the incident radiation at the sea surface is a function of the solar inclination angle and of the scattering and absorption properties of the atmosphere; it has been estimated from the cosine of the solar zenith angle θ, which depends on the day of the year, time of day, and latitude of the site of interest.

The spectral distribution of the solar flux at the top of the atmosphere is based on Neckel and Labs' data (Neckel and Labs, 1984); a spectral resolution of 1 nm is retained throughout the propagation to the sea surface and into the ocean interior.

Under clear skies the direct (E_{dd}) and diffuse (E_{ds}) components of the global downwelling irradiance (E_d) at the sea surface are computed assuming a vertically homogeneous atmosphere. Molecular scattering (Rayleigh scattering) determination is based on measured pressure, ozone, oxygen and water vapour absorption coefficients taken from Bird and Riordan (Bird and Riordan, 1986); aerosol scattering computation is based on an empirical model (Gathman, 1983). We also included Reed's formula (Reed, 1977) to perform simulations with different levels of cloudiness.

This parameterization, however, does not adequately capture the narrow time interval before sunrise and after sunset ($\theta > 90°$, the twilight), during which the upper atmosphere continues to diffuse and to reflect sunlight to the earth's surface. This twilight period has been shown to play a key role in higher plant photoregulation responses (Casal *et al.*, 1990) and in circadian rhythms among plants and animals (Roenneberg and Foster, 1997). The duration of twilight varies with the latitude of the observer and the declination of the sun. To reproduce the surface solar irradiance at zenith angles >90°, we developed an empirical parameterization of the spectral irradiance at zenith angles from 80 to 96°, based on measured values of spectral downwelling irradiance $E_d(\lambda)$ at the sea surface, taken over the twilight period.

The rate of E_d decrease at dusk varies with wavelength, and a second-degree polynomial equation in time captures 99% of the observed variability. The coefficients of the polynomial are computed at each wavelength, subject to the constraint of the value and the first derivative at 80°, as computed based on a $\cos(\theta)$ dependence, and a value of 2.5×10^{-5} W m^{-2} nm^{-1} at 96° for all the wavelengths, which is the limit of sensitivity of the radiometer used (noise equivalent irradiance). It is worth mentioning that the error in the cosine response of the radiometer for $60° < \theta < 85°$ is below 10% and that for $\theta > 90°$ only the diffuse component of downwelling radiation is present. The numerical procedure is applicable to all sites, once the atmospheric properties have been parameterized.

Parameterization of underwater attenuation

The fraction of irradiance transmitted through the sea surface, $E_d(0^-)$ is calculated taking into account the reflection, the refraction and the sea surface roughness (Gregg and Carder, 1990).

The global (direct, E_{dd}, plus diffuse, E_{ds}) downwelling irradiance, E_d, at a given depth z is derived through the following relationship (Sathyendranath and Platt, 1988):

$$E_d(\lambda, z) = E_{dd}(\lambda, z') \cdot e^{-K_{dd}(\lambda,z)\cdot(z-z')} + E_{ds}(\lambda, z') \cdot e^{-K_{ds}(\lambda,z)\cdot(z-z')}$$

where z' is a depth where E_{dd} and E_{ds} are known, and $K_{dd}(\lambda, z)$ and $K_{ds}(\lambda, z)$ are the spectral diffuse (or vertical) downward attenuation coefficients for the direct and the diffuse components of the global downwelling irradiance, respectively.

When it is needed (i.e. for chlorophyll fluorescence computation) scalar irradiance, E_0, is derived as follows:

$$E_0(z, \lambda) = \frac{E_d(z, \lambda)}{\bar{\mu}_d(z, \lambda)}$$

where $\bar{\mu}_d$ is the downwelling average cosine, estimated according to the approximation of Gordon (Gordon, 1989).

The values for K's coefficients derive from an estimate, at 1 m resolution, of the main processes responsible for the attenuation of light in the marine environment: absorption by seawater, phytoplankton, detritus and yellow substance (the coloured dissolved matter, CDOM), backscattering by seawater and particulate matter.

In the version used for the simulations reported in the following sections, the spectral absorption and backscattering coefficients are computed according to bio-optical models used for case I waters, where the variability in optical properties is largely due to variability of phytoplankton. Therefore, the optical properties of the dissolved and particulate matter are parameterized as a function of the concentration of chlorophyll *a*.

In particular the total spectral absorption coefficient, $a(\lambda)$, is derived as proposed by Morel (Morel, 1991).

$$a(\lambda) = [a_w(\lambda) + 0.06 \cdot a_c'(\lambda) \cdot C^{0.65}] \cdot [1 + 0.2 \cdot e^{-0.014 \cdot (\lambda - \lambda_0)}]$$

where $a_w(\lambda)$ is the absorption coefficient of pure water, $a_{c'}(\lambda)$ is a non dimensional statistically derived chlorophyll *a* specific absorption coefficient (normalized by the maximum), 0.06 the value given to the maximal optical cross section of chlorophyll *a* ($a^{*\,\max}_{chl}$), C the chlorophyll *a* concentration. Note that the product of $a^{*\,\max}_{chl}$ by $a_{c'}(\lambda)$ is the optical cross section of chlorophyll *a*, $a^*_{chl}(\lambda)$. The last term in brackets accounts for the contribution of the colored dissolved organic matter (CDOM).

For the total backscatter coefficient, $b_b(\lambda)$, the bio-optical model utilized is the following (Morel, 1988):

$$b_b(\lambda) = \frac{1}{2} b_w(\lambda) + \left[0.002 + 0.02 \cdot \left(\frac{1}{2} - \frac{1}{4}\log C\right) \cdot \left(\frac{550}{\lambda}\right)\right] \cdot [0.30 \cdot C^{0.62} - b_w(550)]$$

with b_w being the total scattering coefficient of pure water.

The optical properties of seawater are based on tabulated values (Smith and Baker, 1981; Haltrin and Kattawar, 1991; Pope and Fry, 1997).

Finally, inelastic or transpectral processes taken into account are Raman scattering and chlorophyll *a* fluorescence; they are of particular interest in the range–R:FR ($\lambda > 600$ nm), less energetic, part of the spectrum, where direct solar light is rapidly absorbed by water ($K_d \approx 0.2$–$2\ m^{-1}$). The relationships used to compute the downward Raman irradiance (Marshall and Smith, 1990; Haltrin and Kattawar, 1993) assume an isotropic distribution function for Raman scattering. The irradiance produced by chlorophyll *a* fluorescence has the shape of a Gaussian curve and peaks around 685 nm. This radiant flux is quantified as a function of chlorophyll *a* concentration, its specific absorption coefficient, $a^*_{chl}(\lambda)$, and the value of the quantum yield of fluorescence Φ_f. This diffuse light field is isotropic and its contribution to the plane downwelling irradiance, E_{fd}, is quantified according to the following expression (Maritorena *et al.*, 2000):

$$E_{fd}(z) = \frac{\Phi_f}{4} \cdot \frac{C \int_{400}^{700} E_0(z,\lambda) a^*_{chl}(z,\lambda) d\lambda}{(k - K_d)}$$

where k represents an attenuation coefficient for the irradiance generated by fluorescence and propagating upward.

RESULTS

Model validation

The validation of the in-water model was performed using data measured in open waters (case I) of the Eastern Mediterranean Sea. Pigment profiles and measured surface E_d were used as input for simulations, and measured downwelling irradiance profiles as validation points.

Discrete samples and fluorometric downcasts were coupled to compute the vertical distribution of chlorophyll concentration with a resolution of 1 m. Irradiance profiles were acquired using a 13 channel (400, 412, 443, 470, 490, 510, 531, 555, 590, 619, 665, 685, 700 nm) spectral radiometer (Satlantic Inc., SeaWiFS Profiling Multispectral Radiometer) following standard SeaWiFS protocols (Mueller *et al.*, 1995).

As reported in Figure 1, modelled profiles show good agreement with *in situ* data in most of the bands. The highest errors are displayed in the near-UV blue region (412, 443 nm), where the mean percentage error is ~10% in the first 20 m and ranges between 50 and 70% in the 20–100 m layer. This discrepancy may derive from an inadequate parameterization either of the absorption due to dissolved matter (i.e. CDOM) or of the backscattering of particulates in Mediterranean waters.

Therefore we reduced the observed difference by modifying the parameterization of the absorption of CDOM (a_{CDOM}).

It is generally accepted that a_{CDOM} follows with the wavelength a roughly exponential law, according to the following expression:

$$a_{CDOM}(\lambda) = a_{CDOM}(\lambda_0) \cdot e^{-S(\lambda - \lambda_0)}$$

where S is the slope of the semi-logarithmic expression, and depends on the light reactivity of the chromophores

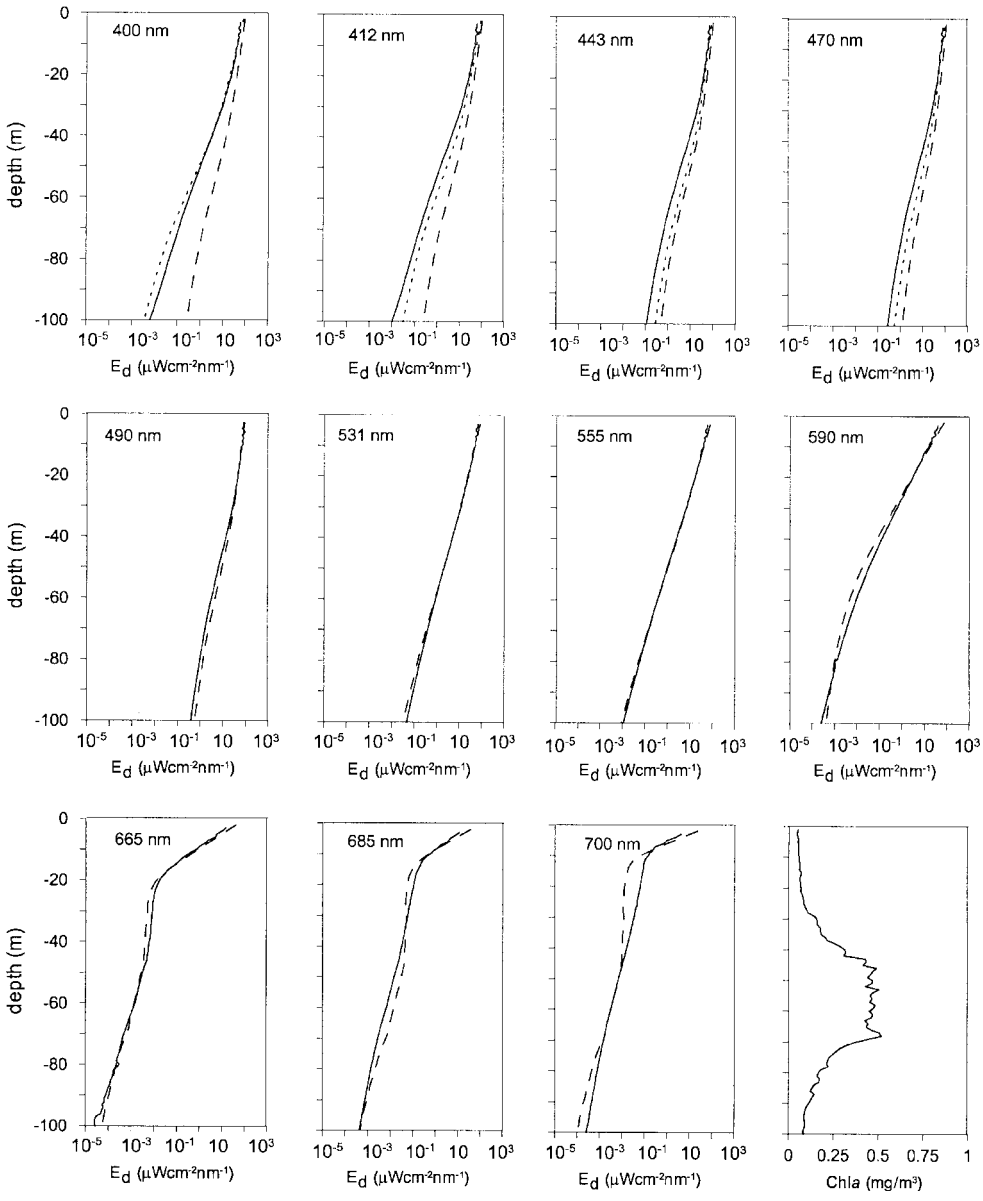

Fig. 1. Vertical profiles of measured (solid line) and modelled (dashed and dotted lines) downwelling irradiance at 11 selected wavelengths in a site of the Eastern Mediterranean Sea. The dashed line refers to the general version of the model, the dotted line to the version modified for the Mediterranean Sea. The chlorophyll profile (last panel) was acquired at the same site and used as input for the simulations.

of the different types of DOM. As shown in the Method section, in the general version of our model S has the constant value of 0.014, following Bricaud *et al.* (Bricaud *et al.*, 1981). Recent studies (Ferrari, 2000) reported higher values (up to 0.028) in the Mediterranean. We found that ~0.05 is the value to use for better reproduction of our *in situ* data (see Figure 1), which is rather high, but close to the upper limit of the range reported for other open-ocean sites (Højerslev and Aas, 2001). Moreover, absorption spectra acquired at several sites in the Mediterranean Sea (WetLab attenuation-absorption meter AC9) seem to confirm what we found numerically, since they in fact exhibit sharp peaks at 412 nm (data not shown), despite what is commonly assumed in case I waters, where phytoplankton are responsible for the highest peak of absorption at 430–440 nm.

Daily and depth variability of band ratios

We quantified the irradiance integrated over selected wave-bands of the visible spectrum, in particular: B

(400–450 nm), G (500–550 nm), R (630–680 nm) and FR (700–750 nm), and analysed the diurnal and vertical variability of the band ratios R:FR, B:R, G:R.

In Figure 2 we report the results of simulations performed at the surface level and at selected depths of the water column. At the sea surface all the analysed band ratios display the highest variability at twilight. In particular, R:FR (Figure 2a) shows a steep increase before dawn followed by a slighter decrease, a rather constant value during the central part of the day, and a symmetric behaviour around dusk. The vertical distribution of the band ratios depends on the optical properties of water and its constituents (suspended and dissolved matter). In water R:FR shows a high degree of daily variability. Its value increases with depth, due to the stronger diffuse attenuation coefficient (K_d) of FR versus R. Nevertheless this variability is observed only in the upper 10–15 m. Below this level, solar incoming irradiance in the 650–750 band is completely lost by water attenuation, and the only R and FR photons present are produced by transpectral

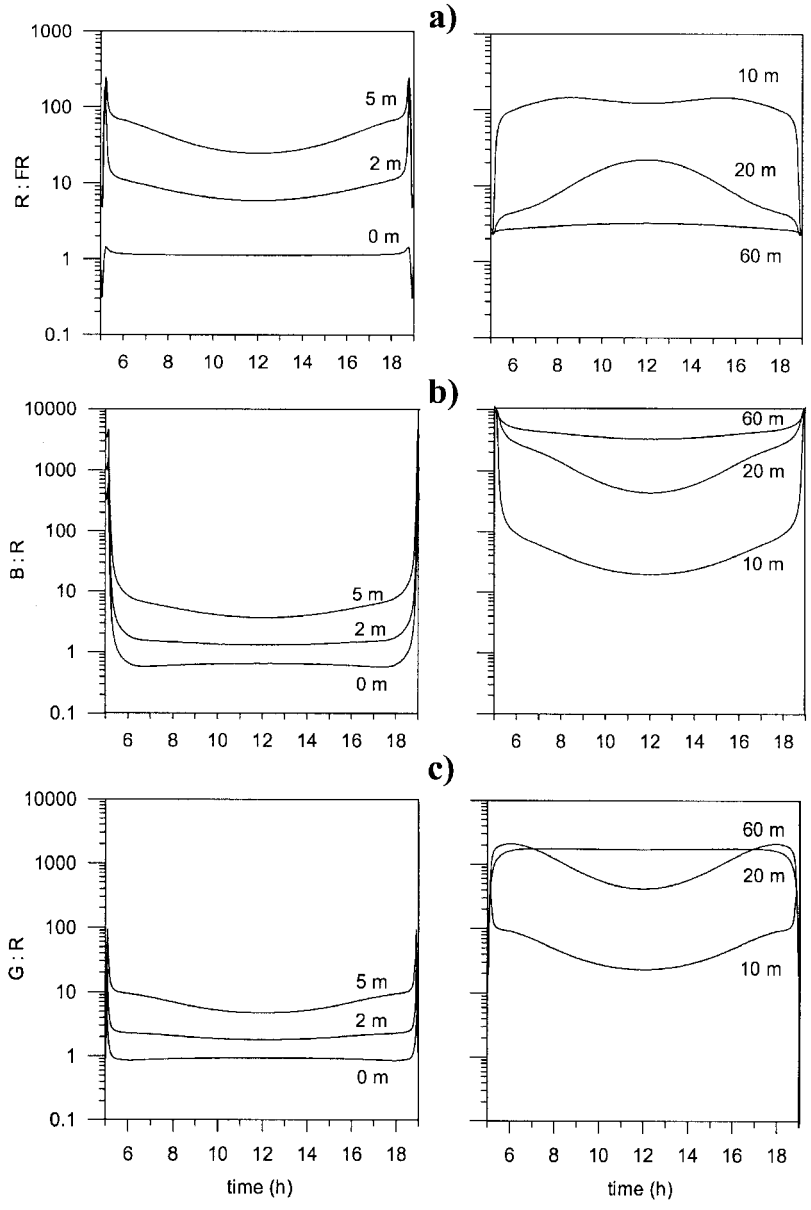

Fig. 2. Band ratio variation with time of the day at selected depths of the water column (note the different scales on the *y*-axis). Chlorophyll concentration as in Figure 1. Irradiance has been integrated over 50 nm per each indicated band. (**a**) R:FR (630–680:700–750. (**b**) B:R (400–450:630–680). (**c**) G:R (500–550:630–680).

processes, i.e. Raman scattering and chlorophyll *a* fluorescence. In addition the R:FR ratio is rather insensitive to the chlorophyll the concentration, as shown in Figure 3a.

Because of the high difference in the attenuation coefficient of B and G versus R light, B:R and G:R ratios reach values up to several thousands as depth increases to 40–50 m (Figure 2b and c). They also display drastic changes on the daily scale, especially at dawn and dusk, observable even at depth.

Finally both ratios are affected by the vertical shape of the chlorophyll profile, exhibiting an evident minimum in correspondence to the chlorophyll maximum (Figure 3b and c); moreover, B:R varies significantly along with changes in concentration of chlorophyll *a*.

The impact of chlorophyll fluorescence

In Figure 3d, R and FR irradiance are reported in relation to chlorophyll *a* concentration. Simulations were performed using modelled pigment profiles with a Gaussian shape, a deep chlorophyll maximum (DCM) located at 50 m with concentrations ranging from 0.3 to 12 mg m^{-3}, constant values for optical cross-section of chlorophyll *a* [$a^{*}_{chl}{}^{max}$ = 0.06 m^2 (mg Chl *a*)$^{-1}$],

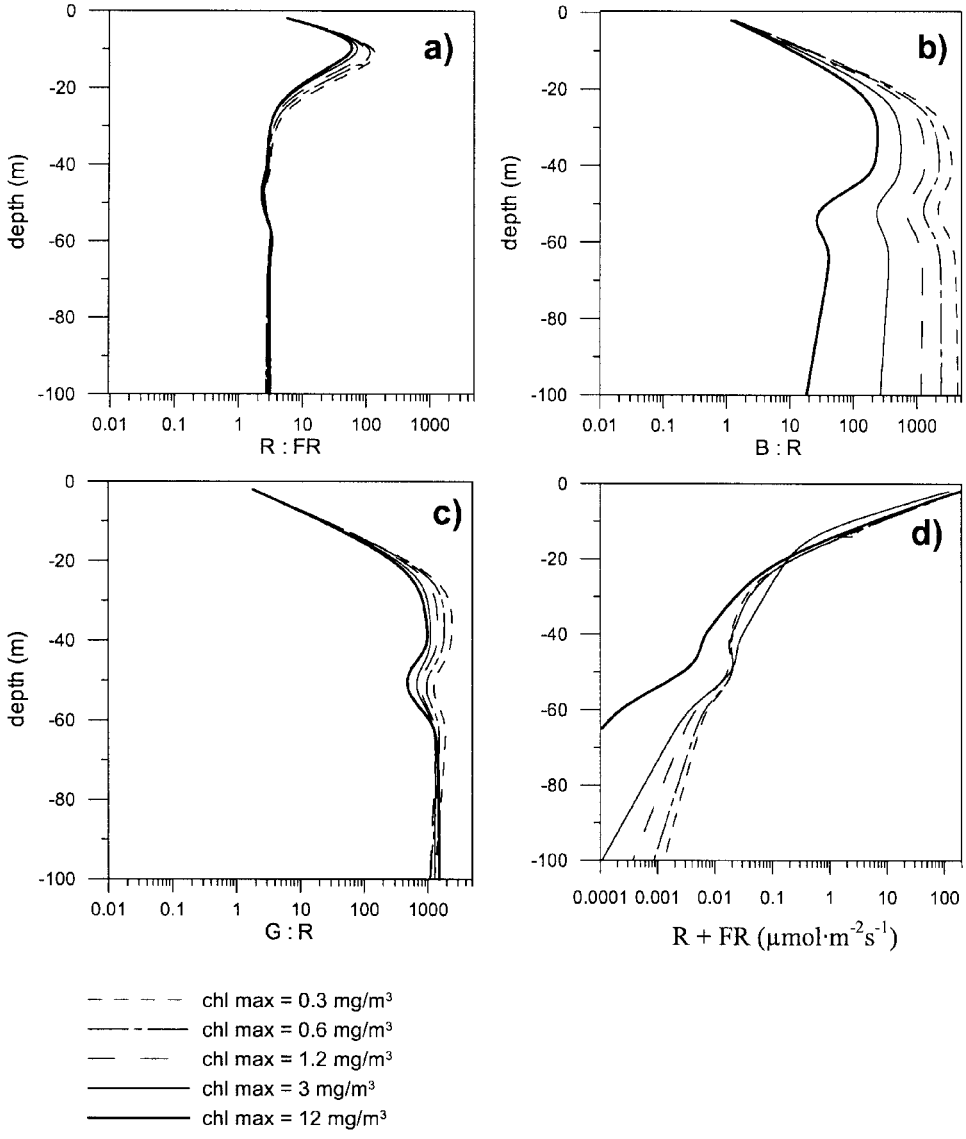

Fig. 3. Vertical profiles of spectral bands at different levels of chlorophyll *a* concentration (chlorophyll maximum at 50 m). (**a**) R:FR ratio (630–680:700–750). (**b**) B:R ratio (400–450:630–680). (**c**) G:R ratio (500–550:630–680). (**d**) R + FR (630–680 + 700–750).

fluorescence quantum yield ($\Phi_f = 0.02$) and solar zenith angle (15°). The resulting R + FR photon irradiance (integrated over 100 nm) incident at the depth of the DCM varies from 1.98×10^{-2} to 2.73×10^{-3} µmol quanta m^{-2} s^{-1} and from 2.39×10^{-3} to 1.31×10^{-6} µmol quanta m^{-2} s^{-1} at 100 m, depending on the total amount of chlorophyll. Indeed R–FR irradiance decreases as pigment content increases, since the absorption of B–G light due to more abundant phytoplankton in fact reduces the available excitation energy.

We also tested the influence of the variability of physiological parameters such as a^*_{chl} and Φ_f on the fluorescence emission. We considered two cases of vertical chlorophyll distribution: the first with a minimum value of 0.1 mg m^{-3} and DCM concentration of 0.4 mg m^{-3}, the second with concentrations 10 times higher (1–4 mg m^{-3}). The results of the analysis are reported in Figure 4 for the depth of the DCM, i.e. 50 m. Over the range considered for Φ_f (0.01–0.06), R + FR irradiance varies ~4-fold in the first case and 5-fold in the second (Figure 4a). On the other hand a positive variation of the optical cross-section has two opposite effects: it increases the fluorescence emission proportionally, but decreases the depth-integrated PAR, thus reducing the amount of fluorescence produced locally. The two effects in some way compensate for each other in the case of DCM = 0.4 mg m^{-3}, so that at the depth of 50 m one can measure similar amounts of R and FR over the range of $a^{*\,max}_{chl}$ considered [0.02–0.12 m^2 (mg Chl *a*)$^{-1}$], with PAR irradiance varying almost 4-fold (Figure 4b). In the case of higher chlorophyll content in the water column, the second effect prevails, thus R and FR decrease by~20-fold as $a^{*\,max}_{chl}$ increases from 0.02 and 0.12 m^2 (mg Chl *a*)$^{-1}$ (Figure 4b), due to a significant reduction in local PAR (from ~52 to 0.7 µmol m^{-2} s^{-1}), which means that the ratio between R and PAR shows variations of 3.5 or 4.5 times (depending on the chlorophyll concentration).

Finally we estimated the red fluorescence generated by a single phytoplankton cell and compared it with the background irradiance in the same band (results reported in Figure 5). The light emitted by a cell having a chlorophyll *a* content of 1 pg ranges from 3.6×10^9 to 5.7×10^{10} photons m^{-2} s^{-1} when locally incident PAR varies from 4.1×10^{18} to 4.9×10^{19}. The rate of arrival of red photons on a neighbour cell is a function of the distance between the 'source' and the 'target' and its size. It ranges from 20 to 0.25% of the emitted flux, as the distance between the two cells varies from 10 to 100 µm. Therefore, in proximity to the DCM, the flux perceivable by one cell due to the emission of another one 100 µm away is 1–3 orders of magnitude greater than the background red light field, depending on the chlorophyll *a* concentration in the water column (Figure 5). Obviously higher or lower cellular pigment content makes the signal from the cell increase or decrease accordingly.

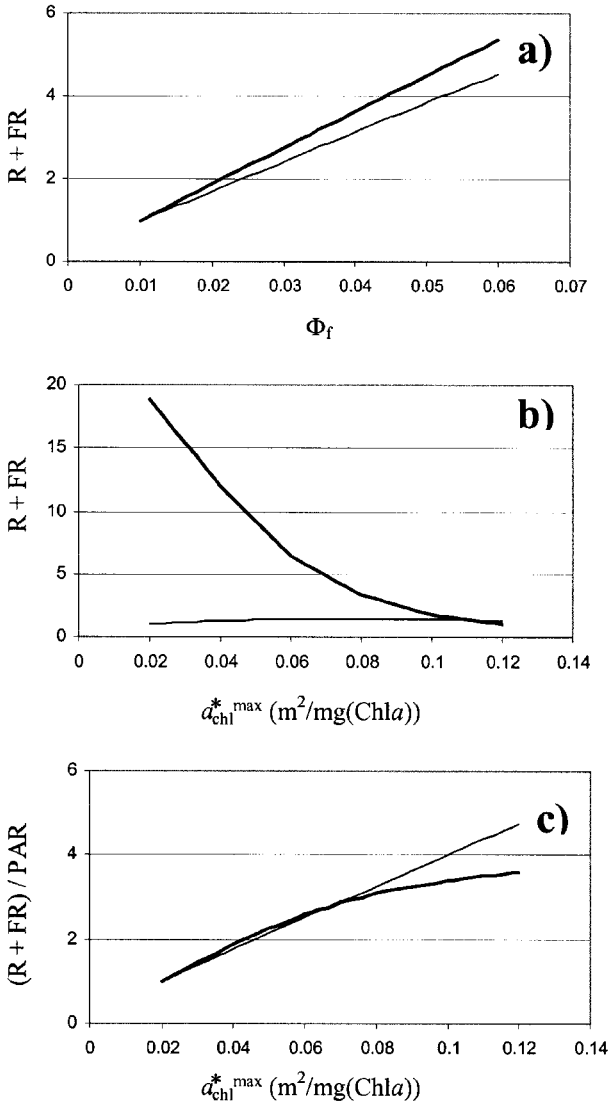

Fig. 4. R + FR irradiance variation with fluorescence quantum yield (Φ_f) and optical cross-section of chlorophyll *a* ($a^{*\,max}_{chl}$) at the depth of DCM, with concentration of 0.4 mg m^{-3} (thin line) and 4 mg m^{-3} (thick line). (**a**) and (**b**) R + FR irradiance is normalized by its minimum value. (**c**) R + FR irradiance is normalized by PAR irradiance.

DISCUSSION

The purpose here was to single out spectral bands and ratios that may contain information on the characteristics of the local environment of marine autotrophs and to formulate testable hypotheses on their ecological significance, based on the results of a radiative transfer model.

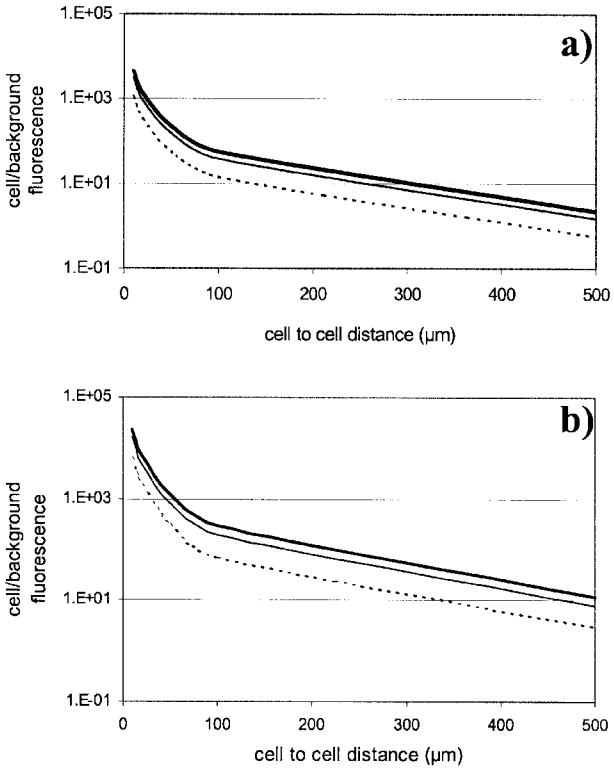

Fig. 5. Ratio of cell to background fluorescence (660–710 nm) as a function of the distance between two cells and of the cellular chlorophyll *a* content. Cellular chlorophyll *a* content: (thick line) 9 pg cell^{-1}; (thin line) 5 pg cell^{-1}; (dotted line) 1 pg cell^{-1}. Simulations were performed with $a^{*}_{chl}{}^{max} = 0.06$ m^2 [mg (Chl *a*)]$^{-1}$ and $\Phi_f = 0.02$. Estimates and parameters reported below refer to the depth of the DCM (50 m). (**a**) Background chlorophyll *a* concentration = 0.4 mg m^{-3}; PAR irradiance = 4.9×10^{19} photons m^{-2} s^{-1}. (**b**) Background chlorophyll *a* concentration = 4 mg m^{-3}, PAR irradiance = 4.1×10^{18} photons m^{-2} s^{-1}.

While the date and the latitude determine only the maximal irradiance and the duration of the twilight, the daily variability of the sun angle also induces a spectral variability in the light field. At dusk and dawn a greater extinction of yellow–orange and a greater transmission of B:G and FR bands occur than in normal daylight. The most relevant aspect of the light pattern in this part of the day is its informational content. In fact, phytochromes of higher plants allow the detection of variations in the R:FR ratio, which represent a signal for the starting and the ending of the photoperiod or for the shading under canopies (Smith, 2000). Indeed, phytochrome-like photoreceptors have also been found in cyanobacteria (Lamparter *et al.*, 1997) and unicellular green algae (Wu *et al.*, 1997; Jorissen *et al.*, 2002), even though their role in the ecological context is still not fully understood, given the high attenuation rate of red light at sea. Green and blue photoreceptors are known to be involved in processes such as phototaxis in flagellate algae (Hader and Lebert, 1998; Sineshchekov and Govorunova, 2001) and chloroplast migration in diatoms and green algae (Kraml and Herrman, 1991; Furukawa *et al.*, 1998). Nevertheless, an overall reassessment of the informational content of the light spectrum and of the role of photoreceptors in the marine environment is still lacking.

We focused on the absorption bands of known and putative photoreceptors of algae and studied their daily and vertical variability, trying to generalize with a different approach the results and the hypotheses emerging from the above mentioned studies.

The significance of light quality ratios as signals is also supported by the presence and the co-action in some marine algae of more than one photoreceptor, such as phytochrome and cryptochrome or phytochrome and green receptors, or green and blue receptors (Ruyters, 1988; Lopez-Figueroa and Niell, 1989).

The daily pattern of R:FR resulting from our simulations had already been reported (Chambers and Spence, 1984; Lopez-Figueroa, 1992), based on *in situ* measurements performed above the sea surface and in coastal waters at very shallow depths (1–3 m). The same authors pointed out that R:FR shifts underwater are greater than those displayed above the surface, and theoretically large enough to provide photoperiodic information. Nevertheless this variability holds only in the upper 10–15 m. Moreover fluctuations in meteorological conditions such as sun glitter, clouds, sea roughness, etc. may change the dependence of band ratios on solar angle. Further study is required on the effect of these and other factors on the daily variability of the underwater light spectrum.

For this reason we quantified the amount of R:FR light over the different scales and conditions in order to establish whether and where, besides the upper 10–15 m, this radiation is in principle perceivable by marine phytochromes. Our estimates at depth with low chlorophyll concentrations agree with downwelling irradiance profiles measured in oligotrophic waters by us (data not shown and Figure 1) and with the hyperspectral radiometric data published by Maritorena (Maritorena *et al.*, 2000). Those estimates of R and FR light intensities suggest additional hypotheses on the assessment of the potential role of phytochrome in marine environment. The classical phytochrome-mediated responses have been denoted very low fluence response (VLFR), low fluence response (LFR) and high irradiance response (HIR), depending on the fluence requirements, in terms of the number of photons received and not of the rate of reception. Hence, considering that VLFRs require photon fluence between 100 pmol m^{-2} and 100 nmol m^{-2} (Mancinelli, 1994), one can say that in oligotrophic waters such responses are possible within the whole euphotic zone, if integrated fluxes over 10 min are considered.

Let us now discuss how the described spectral variation matches the reported photoresponses.

Phototaxis towards red light is often reported as negative (Kondou *et al.*, 2001). The most obvious interpretation of this behaviour is related to the avoidance of supersaturating irradiance regimes. Thus, red light would inform of the proximity to the surface, where photodamage processes are likely to occur. On the other hand, the surface can also be a place 'where to go' for exploiting favourable light conditions; therefore solar red light could have a role in the control of swimming velocity, gravitaxis and chloroplast orientation, in accordance with observations reported in green algae (Kraml and Herrman, 1991; Sineshchekov *et al.*, 2000).

Moreover phytoplankton chlorophyll, as demonstrated above, emits red light perceivable locally by neighbour cells over the background signal.

Due to the short distances (10–100 μm) required for the detection of such a signal, neighbour perception could be relevant only in the case of extremely proximal cells. Recent studies on the diatom *Chaetoceros decipiens* (Pickett-Heaps, 1998) have shown that colony length regulation is a highly controlled process, where the generation of terminal cells, which are morphologically different from the intercalary ones, should depend on external or internal triggers. We hypothesize that one such trigger may in fact be the amount of red fluorescence produced by the other cells in the colony which would allow an estimate of the length of the colony. Furthermore, the detection of ultra-neighbour free cells would significantly help the partitioning of the space at the microscale, preventing the competition for the same resources (e.g. nutrients). As a matter of fact, phototaxis performed by microscopic plankters produces displacements in the same order as cell size, which hardly result in significant changes in the 'macroscopic' light field experienced.

At a larger scale (metres) reductions in B:R and G:R ratio occur at high values of chlorophyll concentration. The related information on the bloom density could then be involved, among other factors, in triggering and timing processes in phytoplankton strategies, such as induction of resting stages (Eilertsen *et al.*, 1995), aggregation (Roenneberg, 1996) and sexual reproduction (gamete formation) (Kremp and Heiskanen, 1999). Indeed, the existence of sharp vertical gradients of chlorophyll fluorescence at fine scales (1–10 m) and microscale (<1 m) is well known (Alldredge *et al.*, 2002), whereas the mechanisms responsible for the formation, maintenance and destruction of those thin layers are still poorly understood. In this context, local density information detected by phytoplankton may have a role, since processes like phototaxis and aggregation occur on temporal and spatial scales compatible with those of such structures.

Finally the classical 'shade-avoidance' responses of higher plants may be also active in phytobenthos which, perceiving red fluorescence from marine plants or macroalgae, could avoid their shade by sliding on the substrate (Cohn and Weitzell, 1996).

In conclusion, in the first 10–15 m of the water column it is possible that marine red photoreceptors mimic the role they play in higher terrestrial plants.

Thus it seems reasonable to hypothesize that the classical phytochrome-mediated responses are more likely to be observed in marine plants and macroalgae, or in phytoplankton of shallow aquatic environments.

Even below that depth there are sufficient amounts of red photons to give a selective advantage to organisms equipped with red photoreceptors. We showed that the perception of red light, whether or not coupled with blue or green radiation, might act to control relevant biological responses, although their trigger is still unknown.

ACKNOWLEDGEMENTS

We wish to thank Chris Bowler and Angela Falciatore for the stimulating discussions we have had on the topic of this paper during the last 3 years, and Marlon Lewis for critically reviewing the manuscript and for his remarkable help in streamlining it.

REFERENCES

Alldredge, A. L., Cowles, T. J., MacIntyre, S., Rines, J. E. B., Donaghay, P. L., Greenlaw, C. F., Holliday, D. V., Dekshenieks, M. M., Sullivan, J. M. and Zaneveld, J. R. V. (2002) Occurrence and mechanisms of formation of a dramatic thin layer of marine snow in a shallow Pacific fjord. *Mar. Ecol. Prog. Ser.*, **233**, 1–12.

Bird, R. E. and Riordan, C. (1986) Simple solar spectral model for direct and diffuse irradiance on horizontal and tilted planes at the earth's surface for cloudless athmospheres. *J. Climatol. Appl. Meteorol.*, **25**, 87–97.

Bricaud, A., Morel, A. and Prieur, L. (1981) Absorption by dissolved organic matter of the sea (yellow substance) in the UV and visible domains. *Limnol. Oceanogr.*, **26**, 43.

Casal, J. J., Sánchez, R. A. and Gibson, D. (1990) The significance of changes in the red/far-red ratio associated either to neighbour plants or to twilight for tillering in *Lolium multiflorum* Lam. *New Phytolog.*, **116**, 565–572.

Chambers, P. A. and Spence, D. H. N. (1984) Diurnal changes in the ratio of underwater red to far red light in relation to aquatic plants photoperiodism. *J. Ecol.*, **72**, 495–503.

Cohn, S. A. and Weitzell, R. E. J. (1996) Ecological considerations of diatom cell motility. 1. Characterization of motility and adhesion in four diatom species. *J. Phycol.*, **32**, 928–939.

Cullen, J. J., Zhu, M., Davis, R. F. and Pierson, D. C. (1985) Vertical migration, carbohydrate synthesis, and nocturna: nitrate uptake

during growth of *Heterocapsa niei* in a laboratory water column. In Anderson, D. M., White, A. W. and Baden, D. G. (eds), *Toxic Dinoflagellates*. Elsevier, New York, pp. 33–38.

Dring, M. J. (1988) Photocontrol of development in algae. *Annu. Rev. Plant Physiol. Plant Mol. Biol.*, **39**, 157–174.

Eilertsen, H., Sandberg, S. and Tollefsen, H. (1995) Photoperiodic control of diatom spore growth: a theory to explain the onset of phytoplankton blooms. *Mar. Ecol. Prog. Ser.*, **116**, 303–307.

Ferrari, G. M. (2000) The relationship between chromophoric dissolved organic matter and dissolved organic carbon in the European Atlantic coastal area and in the West Mediterranean Sea Gulf of Lions. *Mar. Chem.*, **70**, 339–357.

Furukawa, T., Watanaba, M. and Shihira-Ishikawa, I. (1998) Green- and blue-light-mediated chloroplast migration in the centric diatom *Pleurosira laevis*. *Protoplasma*, **203**, 214–220.

Gathman, S. G. (1983) Optical properties of the marine aerosols as predicted by the Navy aerosol model. *Opt. Eng.*, **22**, 57–62.

Gordon, H. R. (1989) Can the Lambert–Beer law be applied to the diffuse attenuation coefficient of ocean waters? *Limnol. Oceanogr.*, **34**, 1389–1409.

Gregg, W. W. and Carder, K. L. (1990) A simple spectral solar irradiance model for cloudless maritime atmospheres. *Limnol. Oceanogr.*, **35**, 1657–1675.

Grossmann, A. R., Shaefer, M. R., Chiang, G. G. and Collier, J. L. (1993) Environmental effects on the light-harvesting complex of cyanobacteria. *J. Bacteriol.*, **175**, 575–582.

Hader, D.-P. and Lebert, M. (1998) The photoreceptor for phototaxis in the photosynthetic flagellate *Euglena gracilis*. *Photochem. Photobiol.*, **68**, 260–265.

Haltrin, V. I. and Kattawar, G. W. (1991) Light fields with Raman scattering and fluorescence in sea water. Technical Report. College Station, Department of Physics, Texas A&M University, 74 pp.

Haltrin, V. I. and Kattawar, G. W. (1993) Self-consistent solutions to the equation of transfer with elastic and inelastic scattering in ocean optics: I. model. *Appl. Opt.*, **32**, 5356–5367.

Højerslev, N. K. and Aas, E. (2001) Spectral light absorption by yellow substance in the Kattegat–Skagerrak area. *Oceanologia*, **43**, 39–60.

Hughes, J. E., Morgan, D. C., Lambton, C. R., Black, C. R. and Smith, H. (1984) Photoperiodic time signals during twilight. *Plant Cell Environ.*, **7**, 269–277.

Jorissen, H. J. M. M., Braslavski, S. E., Wagner, G. and Gartner, W. (2002) Heterologous expression and characterization of recombinant phytochrome from the green alga *Mougeotia scalaris*. *Photochem. Photobiol.*, **76**, 457–461.

Kondou, Y., Nakazawa, M., Higashi, S., Watanabe, M. and Manabe, K. (2001) Equal-quantum action spectra indicate fluence-rate selective action of multiple photoreceptors for photomovement of the thermophilic cyanobacterium *Synechococcus elongatus*. *Photochem. Photobiol.*, **73**, 90–95.

Kraml, M. and Herrmann, H. (1991) Red–blue interaction in *Mesotaenium chloroplast* movement—blue seems to stabilize the transient memory of the phytochrome signal. *Photochem. Photobiol.*, **53**, 255–259.

Kremp, A. and Heiskanen, A.-S. (1999) Sexuality and cyst formation of the spring-bloom dinoflagellate *Scrippsiella hangoei* in the coastal northern Baltic Sea. *Mar. Biol.*, **134**, 771–777.

Lamparter, T., Mittmann, F., Gartner, W., Borner, T., Hartmann, E. and Hughes, J. E. (1997) Characterization of recombinant phytochrome from the cyanobacterium *Synechocystis*. *Proc. Natl Acad. Sci. USA*, **94**, 11792–11797.

Lopez-Figueroa, F. (1992) Diurnal variation in pigment content in *Porphyra laciniata* and *Chondrus crispus* and its relation to the diurnal changes of underwater light quality and quantity. *P.S.Z.N.I: Mar. Ecol.*, **13**, 285–305.

Lopez-Figueroa, F. (1998) Diel migration of phytoplankton and spectral light field in the Ria de Vigo (NW Spain). *Mar. Biol.*, **130**, 491–499.

Lopez-Figueroa, F. and Niell, F. X. (1989) Red-light and blue-light photoreceptors controlling chlorophyll *a* synthesis in the red alga *Porphyra umbricalis* and in the green alga *Ulva rigida*. *Physiol. Plant.*, **76**, 391–397.

Mancinelli, A. L. (1994) The physiology of phytochrome action. In Kendrick, R. E. and Kronenberg, G. H. M. (eds), *Photomorphogenesis in Plants*. Kluwer Academic Publishers, Dordrecht, pp. 211–269.

Maritorena, S., Morel, A. and Gentili, B. (2000) Determination of the fluorescence quantum yield by oceanic phytoplankton in their natural habitat. *Appl. Opt.*, **39**, 6725–6737.

Marshall, B. R. and Smith, R. C. (1990) Raman scattering and in-water ocean optical properties. *Appl. Opt.*, **29**, 71–84.

Morel, A. (1988) Optical modeling of the upper ocean in relation to its biogenous matter content (Case 1 water). *J. Geophys. Res. [Oceans]*, **93**, 10749–10768.

Morel, A. (1991) Light and marine photosynthesis: a spectral model with geochemical and climatological implications. *Prog. Oceanogr.*, **26**, 263–306.

Mueller, J. L. and Austin, R. W. (1995) Ocean optics protocols for SeaWiFS validation, Technical Report Series. In Hooker, S. B., Firestone, E. R. and Acker, J. (eds), *NASA Technical Memorandum 104566, Rev., 1*, Greenbelt, MD.

Neckel, H. and Labs, D. (1984) The solar spectrum between 3300 and 12500 Å. *Sol. Phys.*, **90**, 205–258.

Pickett-Heaps, J. D. (1998) Cell division and morphogenesis of the centric diatom *Chaetoceros decipiens* (Bacillariophyceae) I. Living cells. *J. Phycol.*, **34**, 989–994.

Pope, R. M. and Fry, E. S. (1997) Absorption spectrum (380–700 nm) of pure water. II. Integrating cavity measurements. *Appl. Opt.*, **36**, 8710–8723.

Reed, R. K. (1977) On estimating insolation over the ocean. *J. Phys. Oceanogr.*, **7**, 482–485.

Roenneberg, T. (1996) The complex circadian system of *Gonyaulax polyedra*. *Physiol. Plant.*, **96**, 733–737.

Roenneberg, T. and Foster, R. G. (1997) Twilight times: light and the circadian system. *Photochem. Photobiol.*, **66**, 549–561.

Ruyters, G. (1988) Light-stimulated respiration in the green alga *Dunaliella tertiolecta*: involvement of the ultrviolet/blue-light photoreceptor(s) and phytochrome? *Planta*, **174**, 422–425.

Sathyendranath, S. and Platt, T. (1988) The spectral irradiance field at the surface and in the interior of the ocean: a model for applications in oceanography and remote sensing. *J. Geophys. Res. [Oceans]*, **93**, 9270–9280.

Senger, H. and Bauer, B. (1987) The influence of light quality on adaptation and function of the photosynthetic apparatus. *Photochem. Photobiol.*, **45**, 939–946.

Sineshchekov, O. and Govorunova, E. G. (2001) Rhodopsin receptors of phototaxis in green flagellate algae. *Biochemistry*, **66**, 1300–1310.

Sineshchekov, O., Lebert, M. and Hader, D.-P. (2000) Effects of light on gravitaxis and velocity in *Chlamydomonas reinhardtii*. *J. Plant Physiol.*, **157**, 247–254.

Smith, H. (2000) Phytochromes and light signal perception by plants—an emerging synthesis. *Nature*, **407**, 585–591.

Smith, R. C. and Baker, K. (1981) Optical properties of the clearest natural waters. *Appl. Opt.*, **20**, 177–184.

Sournia, A. (1974) Circadian periodicities in natural populations of marine phytoplankton. *Adv. Mar. Biol.*, **12**, 325–389.

Wu, S.-H. and Lagarias, J. C. (1997) The phytochrome photoreceptor in the green alga *Mesotaenium caldariorum*: implication for a conserved mechanism of phytochrome action. *Plant Cell Environ.*, **20**, 691–699.

Received on July 23, 2003; accepted on January 27, 2004; published online on February 16, 2004